

Corneal Topography and Tomography

15

Jaime Aramberri

Introduction

Corneal optics determines the optical performance of the eye. The present day intraocular lens (IOL) technologies and the high expectations of cataract and refractive lensectomy patients demand an exhaustive preoperative analysis of corneal shape and optics with latest generation tomographers. In this way, corneal optics can be evaluated further beyond simple keratometry; any irregularity described in terms of aberrometry, the possibility of later laser refractive treatments ascertained, and other subtle problems that could affect visual function can be detected. This diagnostic method has become by its own right the cornerstone of IOL selection in lens surgery.

There has been a significant evolution from Placido topographers, where only the anterior corneal surface is analyzed, to elevation tomographers that can also measure corneal thickness and the posterior surface rendering a total corneal assessment. The early devices were based on scanning-slit technology, then on Scheimpflug imaging, and more recently on optical coherence tomography (OCT). At present, corneal tomography is a powerful tool that provides essential

information about the cornea in order to help select the type of IOL, calculate its power and toricity accurately, and estimate the final visual quality. This helps the surgeon to maintain a tight control of the process.

Technologies

Reflection Topography

This method studies the shape of the anterior corneal surface from the analysis of the size of the image of a test mire pattern projected from a known distance. Nearly all commercial devices use a pattern composed of alternating black and white rings called a Placido disk [1] (Fig. 15.1a). Some instruments use color rings to improve the identification of boundaries which can be useful in case of irregular corneas where there might be edge overlapping. The Cassini[®], Ioptics, topographer uses a multiple dot color pattern instead of concentric rings [2] (Fig. 15.1b).

Placido mires are normally non-planarly arranged, inside a rotationally symmetric aspherical surface to achieve a wide-angle ring projection and to obtain an image reflected onto one plane so that the central CCD camera gets a sharp image. Instruments can be classified as small-target (cone topographer) and large-tar-

J. Aramberri (✉)
Clínica Miranza BEGITEK, San Sebastián, Spain
Clínica ÓKULAR, Vitoria, Spain

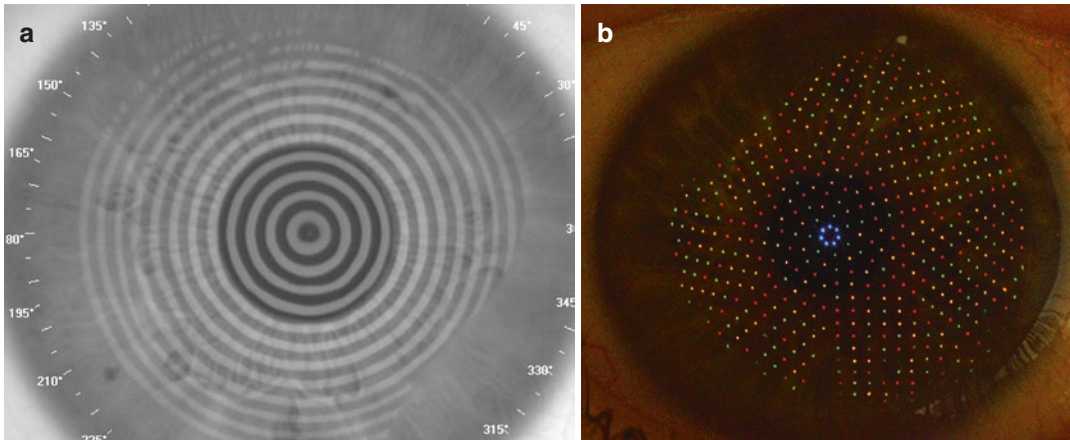


Fig. 15.1 Reflection topography test mires. (a) Placido rings and (b) Cassini color dot pattern

get (disk topographer). In the former, the ring pattern is arranged in a small highly curved surface and the projecting distance is small, while in the latter the projecting surface has smaller curvature and the working distance is longer [3]. These configurations allow covering a wide field of cornea, 8–10 mm, and measuring around 6000–15,000 points depending on the instrument. In IOL power calculation, the area of interest is the central, so-called optical cornea.

The image is captured by a digital camera in a short period of time and first processed by ring boundaries identification. The software reconstructs the corneal shape with a proprietary algorithm. The accuracy and precision of each device will depend on this hardware–software combination. Most topographers use arc-step algorithms that trace arcs sequentially, dot by dot, from the corneal vertex to the periphery. They have been proven to be more accurate in height and instantaneous curvature calculation than old algorithms that assumed a spherical geometry, with less than 0.25μ error in the central 3 mm [4].

In reflection topography, a small distance between rings (or dots) means a steep curvature and vice versa. Any corneal surface or tear film irregularity will translate into ring irregularity. A visual check of the Placido ring image provides some qualitative information about the corneal surface and/or tear film (Fig. 15.2).

Cassini is a unique reflection topographer in that it uses a multiple dot color pattern (679 LEDs) that facilitates a true object-image correspondence decreasing reconstruction errors in case of skew rays [5]. This is especially important when the cornea is not rotationally symmetric, for example, astigmatism, especially if it is irregular. This device can also measure posterior corneal keratometry from the reflection of a ring of dots produced by seven infrared LEDs.

Elevation Topography

The advent of technologies that can obtain cross-sectional images of the cornea allowing simultaneous anterior and posterior corneal topography represented a quantum leap in corneal diagnostics. These instruments project some light on the cornea and record corneal sections in different meridians from the backscattered light (Rayleigh scattering) (Table 15.1).

- *Scanning slit*: In 1995, the Orbscan® topographer, Orbtex, was the first to use a slit of light that scanned horizontally the cornea assessing both corneal surfaces. In 1999, it evolved to Orbscan II®, Bausch & Lomb, incorporating a Placido disk to increase its accuracy in anterior corneal measurement [6].
- *Scheimpflug*: In 2003, Pentacam®, Oculus, was the first corneal tomographer that used the

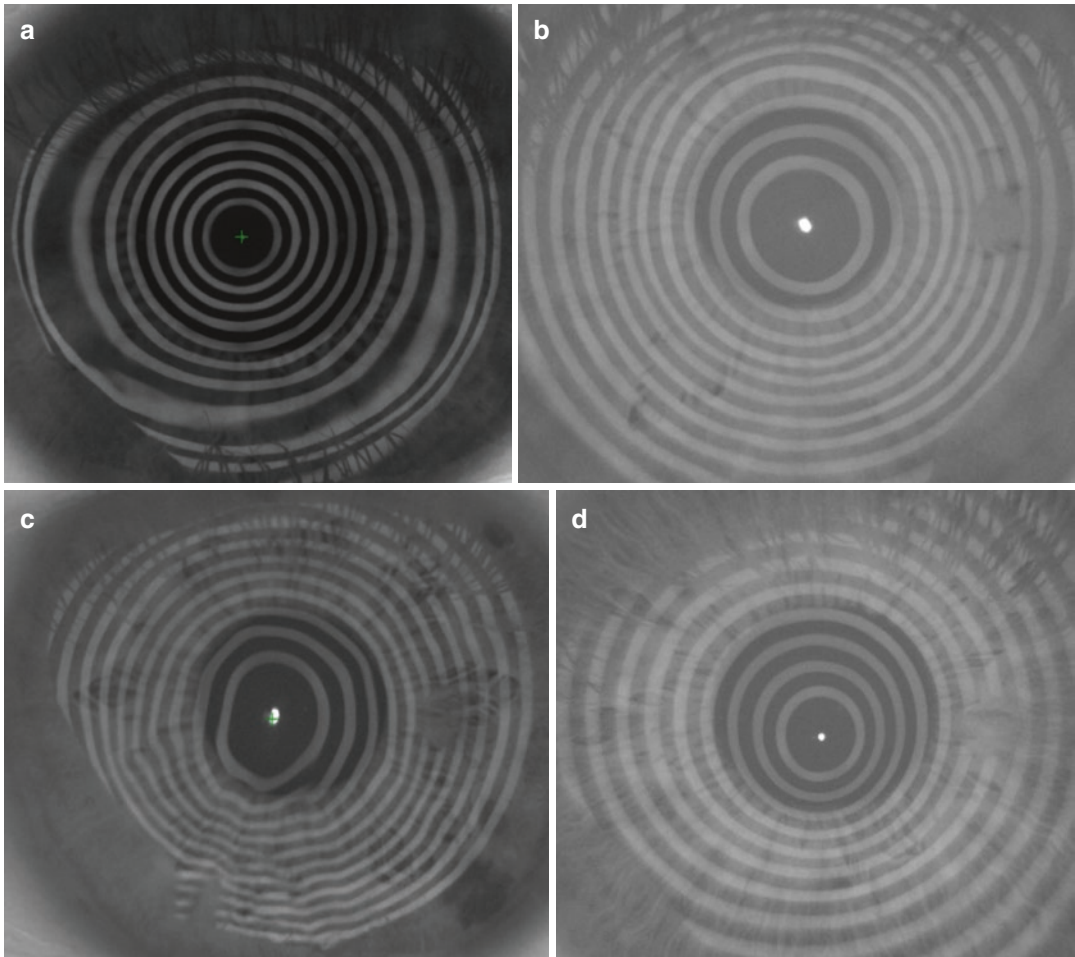


Fig. 15.2 (a) Central thin rings in a steep cornea ($K = 48$ D). (b) Central thick rings in a flat cornea ($K = 34$ D). (c) Irregular rings in a case of corneal scar. (d) Paracentral inferior steepening in a case of keratoconus

Table 15.1 Scheimpflug and OCT corneal tomographers

Technology	Model	Hardware	Wavelength (nm)	Scan time (s)	Meridians	AL
Scheimpflug	PENTACAM HR/AXL	1 camera	475	2	25	Yes
	GALILEI G4/G6	2 cameras Placido	470	1	60	Yes
	SIRIUS	1 camera Placido	475	1	25	No
	TMS 5	1 camera Placido	475	1	64	No
OCT	ANTERION	Swept source	1300	0.5	65	Yes
	MS39	Spectral Placido	845	1	25	No
	CASIA 2	Swept source	1310	0.3	16	No
	REVO NX	Spectral	830	0.17	16	No



Fig. 15.3 From left to right: (a) Orbscan scanning-slit, (b) MS 39 Placido/FD-OCT, and (c) Casia 2 FD-OCT

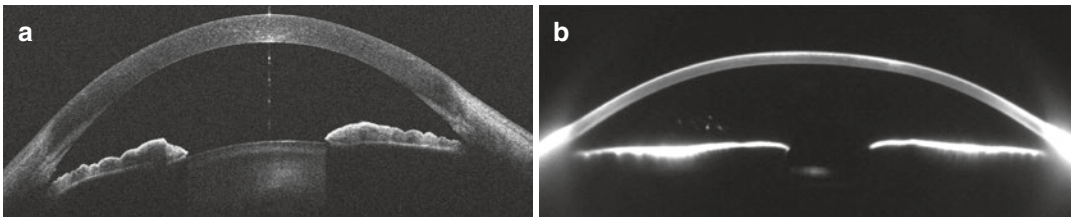


Fig. 15.4 Corneal image by OCT (a) has higher resolution and presents less light scatter with sharper boundaries than Scheimpflug image (b)

Scheimpflug photography principle to analyze the cornea by means of a rotating camera. Later, other instruments using the same principle were marketed: Galilei[®], Ziemer, TMS[®], Tomey, Sirius[®], CSO, etc.

- *Optical Coherence Tomography (OCT)* (Fig. 15.3): This technology has boosted corneal tomography due to a significant improvement in image quality. In 2009, Zeiss commercialized the Visante-Omni[®] that used Time-Domain (TD)-OCT to measure the posterior corneal surface. The anterior topography was measured with a Placido system. The evolution to Frequency-Domain (FD)-OCT technology has

decreased the image acquisition time allowing anterior surface topography from OCT data. At present time, there are three devices that measure both anterior and posterior corneal topography just from OCT data: Casia 2[®] (Tomey), Anterion[®] (Heidelberg), and Copernicus/Revo NX[®] (Optopol). The MS39[®] (CSO) still combines Placido disk for anterior cornea and spectral FD-OCT for the posterior topography.

Compared to other technologies, OCT has increased posterior corneal analysis accuracy due to a significant image quality improvement (Fig. 15.4). OCT has higher axial resolution in

tissue: 5 μm in the case of spectral FD-OCT and 10 μm in the case of Swept Source FD-OCT [7].

Measurements

All devices will describe both corneal surfaces in terms of elevation, curvature, and optical function. Reflection topographers can obtain elevation and curvature information by an arc step calculation method applied to the obtained reflected image, while elevation tomographers will directly get the elevation fitting a curve to the cross-sectional image of the cornea (Fig. 15.5). Afterwards, curvature will be calculated by differentiation.

The relationship between curvature and elevation is a function of the distance to the optical axis. Using a conic function formula, it can be found that the difference in elevation for two curves of 7.85 mm (43 D) and 7.67 mm (44 D) is around 1.5 μm at a distance of 1 mm to the center. This value is under the resolution of any current elevation tomographer, and this is why many instruments, Scheimpflug and OCT, still use a Placido disk to measure the anterior cornea. However, there are other models that rely exclusively on elevation to calculate corneal curvature having shown excellent repeatability and good agreement with other devices [8, 9].

Axial and Tangential Radii

The curvature radius of each surface point can be calculated in two ways [10]:

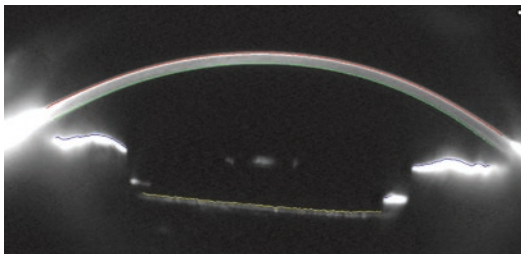


Fig. 15.5 Boundaries identified in a Scheimpflug image (Pentacam). Initial step before best fitting function is calculated

- Axial (sagittal) radius: The distance from the optical axis to the surface normal at that point.
- Tangential (instantaneous, meridional) radius: The distance from the center of curvature of the best fit sphere of each point to the surface normal at that point.

The axial radius only describes adequately symmetrical profiles like the central cornea where the radius of curvature can be assumed to be in the optical axis. Tangential radius will better describe asymmetrical features and the corneal periphery.

Metrics

Three types of metrics are available to the user:

Curvature Metrics

- Radii of curvature: Both axial and tangential radii (in mm) are available in color-coded maps and in indices for different areas of analysis, for example, Sim K, 5 mm semi-meridians.
- Keratometric curvature: Applying the paraxial formula for spheres with the standard keratometric index of refraction (SKIR = 1.3375), the axial and tangential powers are calculated.

$$P = \frac{n_2 - n_1}{r} = \frac{1.3375 - 1}{r} = \frac{0.3375}{r} \quad (15.1)$$

where P is power, n_2 is index of refraction of cornea, n_1 is index of refraction of air, and r is radius of curvature.

This convention has been followed by all manufacturers accepting the heritage of keratometry. The mean value for an annular region of an approximate diameter of 3 mm is known as Sim K (simulated keratometry). There can be small systematic differences among instruments because each one calculates this value in a particular way, for example, Sirius and MS-39 define this value as the mean of the sagittal power from the fourth to the eighth Placido ring (Phoenix 4.0 manual) and Pentacam defines it as the mean

value of a ring 15° around the vertex normal (software 6.10r53). Powers are also calculated for other diameters as well as it has been mentioned above for radii.

Color-coded maps are also displayed where steep areas are represented by long wavelengths (*hot* colors) and flat areas represented by short wavelengths (*cold* colors).

It should be emphasized that keratometric diopters do not represent actual optical power but only curvature: A perfectly spherical cornea with a 7.5 mm curvature radius will be 45 diopters all over the surface. Spherical aberration, higher power in the periphery, is not taken into account.

- Keratometric astigmatism is the difference between the steepest and flattest meridian. It can be expressed as Sim K astigmatism, where both axes are 90° apart, or for other areas of analysis.
- Asphericity index (shape factor): This parameter expresses the rate of change of curvature from the center to the periphery of the cornea for a certain analyzed diameter. It determines the spherical aberration of the aphakic eye. The mean value is available for the anterior and posterior corneal surfaces. Four different coefficients are usually provided: Q , p , e , and E [11].

Elevation Metrics

Measured elevation data are displayed in color-coded maps that express the difference with respect to a certain reference plane. As the cornea is best fitted with an asphero-toric curve, this will be the reference body that will disclose more accurately the tiniest irregularities. Some topographers also describe the surface elevation with a Zernike polynomial expansion.

Refractive Power Metrics

Ray-tracing methodology is used to calculate the actual optical properties of the cornea. An incoming collimated bundle of rays is traced through the anterior and posterior (if measured) corneal surface applying Snell’s law. Some devices use Gullstrand’s refractive indices for cornea (1.376) and aqueous (1.336), while others use proprietary values.

- Refractive power map: the distribution of power is displayed in a color-coded map.
- Refractive power indices: There is no standardization on the name of a central mean total power parameter, and thus each instrument uses a different name for it. The total corneal refractive astigmatism is the difference in total refractive power between the steepest and flattest meridians.
- Wavefront analysis: The anterior, posterior, and total wavefront aberration maps and Zernike coefficients are calculated by all topotomographers. The latter are expressed in RMS values. The wavefront error map represents the difference in height between the corneal wavefront and an ideal wavefront within the analysis diameter.

Precision and Agreement

Central curvature measurement is similar to automated keratometers: the within-subject standard deviation value of repeated measurements around 0.10 D (Sim K) [12]. Placido topographers are usually slightly more imprecise than elevation ones probably due to their tear film quality dependence. Table 15.2 shows different values obtained by our group in different precision studies in healthy eyes presented at IOL Power Club meetings over the past 10 years. The impact of this error level in IOL power calculation is small and can be calculated by Gaussian error propagation analysis: a two-fold increase of Sim K imprecision will barely affect final refraction prediction

Table 15.2 Precision of 3 repeated measurements on healthy eyes in different studies with different topotomographers. S_w within-subject standard deviation from ANOVA. CV coefficient of variation

Device	Year	N	Sim K	S_w	CV
Pentacam HR	2011	35	43.22 ± 1.43	0.06	0.14
MS 39	2019	29	43.88 ± 1.19	0.08	0.17
Casia 2	2017	41	44.05 ± 1.34	0.08	0.17
Galilei G2	2011	35	43.19 ± 1.39	0.10	0.23
IOL master 700	2015	34	43.85 ± 1.79	0.10	0.23
Anterion	2019	29	43.43 ± 1.19	0.12	0.27
Sirius	2017	41	43.94 ± 1.41	0.16	0.37

error and the distribution of cases within ± 0.50 and ± 1.00 D of the prediction (Table 15.3).

Measurement precision will be worse under any circumstance that affects corneal regularity and/or tear film quality: previous corneal surgery, aging, dry eye, etc. [13].

Curvature measurement agreement is fairly good among different technologies and instruments. Most studies report differences between 0.05 and 0.4 D in Sim K. This value can be sig-

Table 15.3 Contribution of Sim K standard deviation, $\sigma(K)$, to the final refraction standard deviation, $\sigma(R_s)$. Calculations performed for three different axial lengths. The last two columns display the proportion of eyes within certain refraction ranges. These standard deviation values have been set constants in the model: AXL = 0.02 mm; ELP = 0.2 mm; IOL = 0.13 D; $n = 0.002$

AXL (mm)	$\sigma(K)$	$\sigma(R_s)$	± 0.50 D	± 1.00 D
23.50	0.1	0.33	87.03%	99.76%
	0.2	0.37	82.34%	99.31%
21.50	0.1	0.42	76.61%	98.27%
	0.2	0.46	72.29%	97.03%
27.00	0.1	0.19	99.15%	100%
	0.2	0.26	94.55%	99.99%

nificant if the parameter is used to calculate IOL power; therefore, it should be measured and compensated for this task. IOL constant optimization for a new device will take this bias into account.

Software

In addition to the regular topographic software, all topo-tomographers integrate specific modules oriented for IOL power calculations, where corneal measurements are combined with biometry values. Four modules can be distinguished:

Surgical Planning Information (Fig. 15.6)

The important metrics are keratometry based data like Sim K and keratometric astigmatism; ray-tracing based refractive power values like total power and total astigmatism; shape factor; Zernike aberrometry coefficients; pupil position

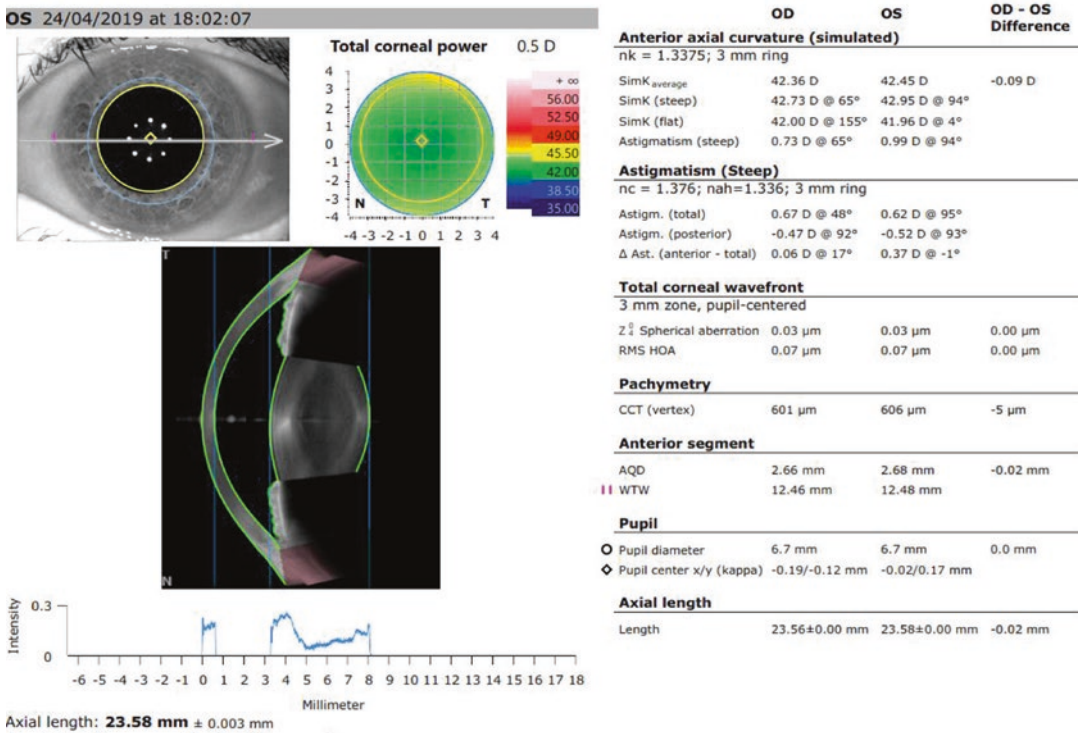


Fig. 15.6 IOL surgery planning module of Anterior tomographer

and diameter; lens thickness (only some devices with PCI and SS-OCT technologies); other biometric parameters like axial length, corneal diameter, corneal thickness, ACD, etc.

IOL Calculation

IOL calculation formulas are programmed in order to perform these calculations. Third-generation formulas like Hoffer Q, Holladay 1, and SRK/T are present in all of them. Newer formulas like Barrett Universal II, Hoffer QST, Kane, RBF, specific post-LASIK formulas like Shammas-PL, and ray-tracing software like Okulix and Phaco-Optics are available only in certain platforms. CSO devices, Sirius®, and MS39® incorporate a proprietary ray-tracing module adequate for odd corneas (post-LASIK, etc.) [14].

Toric IOL Calculations

Tomographers can base their calculations both in keratometric astigmatism and in total corneal astigmatism measured by ray-tracing of anterior and posterior cornea. One of the best-known toric calculators is normally available: Abulafia-Koch, Barrett toric, Holladay 2 toric, Naeser-Savini, etc.

Post-surgical Analysis

Refractive data can be entered to keep track of results and optimize the IOL constant. Some devices can image the rotational position of the toric IOL and calculate the rotation necessary to improve the refractive astigmatism. The Casia 2® has an IOL position analysis module that can measure centration and tilt of the IOL (Fig. 15.7).

Post-op Cataract

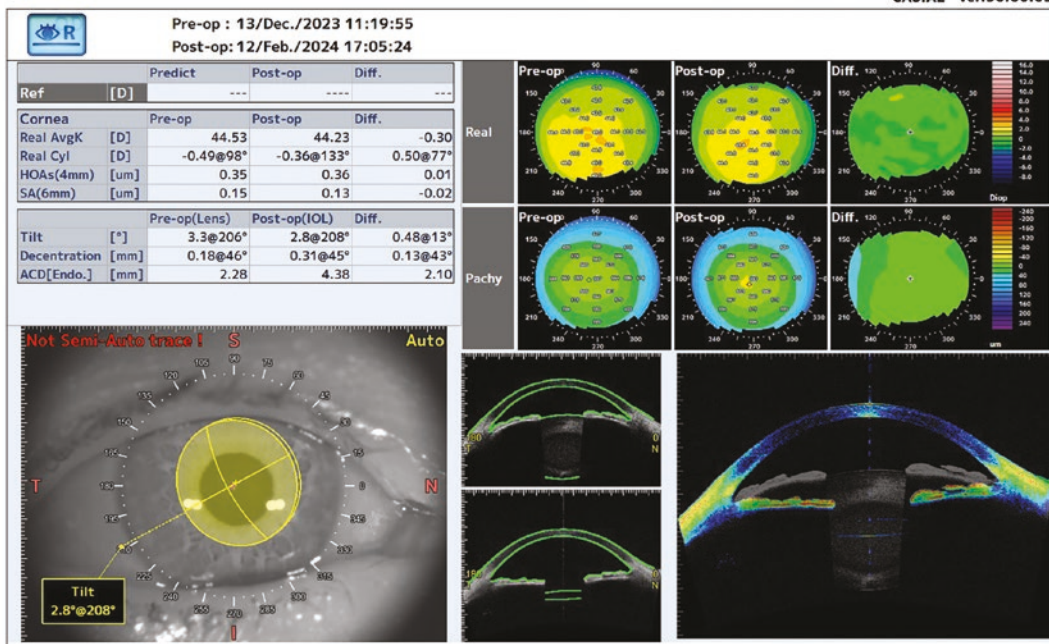


Fig. 15.7 Postoperative analysis module of CASIA 2®

IOL Selection

The IOL selection process implies choosing among different levels of optical performance and compromise, where one design can fit one type of eye but can be contraindicated in another, i.e., a multifocal diffractive IOL can provide good visual quality combined with a regular cornea but not with one that presents a post-LASIK decentered topographical optical zone. The toricity and shape of the IOL are also a matter of consideration in this context. All these decisions are primarily based on corneal topo-tomographic information.

Corneal Optical Quality

Corneal optical quality measurement allows determining if the eye is suitable for the implantation of an IOL design that entails some functional compromise that occurs with many multifocal models. It is also useful to estimate the visual performance after surgery allowing the surgeon to provide the correct information to the patient and define reasonable expectations. This will undoubtedly affect the perceived result and improve the quality of the surgery.

Corneal optical quality is usually assessed by wavefront error aberration analysis. All tomographers present such a software module where Zernike polynomial expansion of the wavefront error is calculated, and some metrics are displayed: Zernike coefficients for several orders, RMS of different combinations of terms (higher and lower order aberrations, HOA and LOA, coma, trefoil, etc.), point spread function, PSF, modulation transfer function (MTF), Strehl ratio, etc. (Fig. 15.8).

Zernike polynomials contribute differently to the overall visual quality. The lower the order and the more central in the pyramid the greater the effect on visual quality. Fourth-order spherical aberration and third-order coma are usually the most relevant HOA values. In aberrated corneas, it is interesting to check the image simulation because the final effect on visual quality will depend on how these terms combine.

There are not universally accepted normality cut-off values. It has been suggested that a relative contraindication for multifocal IOLs is a value over 0.3 μm of corneal HOA in 4 mm diameter, due to equivalency with 0.50 D blur [15]. But there is lack of empirical evidence to support any precise threshold value. Another related issue

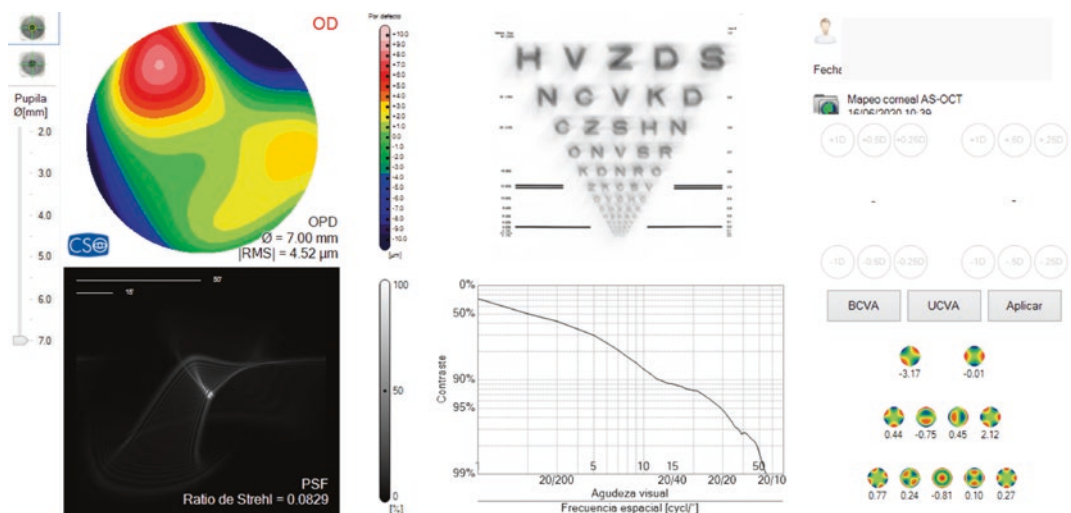


Fig. 15.8 Optical quality display: in the upper row, the wavefront error map (OPD) with some indices and the image simulation. In the lower row, the PSF figure and the

Strehl ratio, the MTF curve and the Zernike coefficients pyramid are displayed

Table 15.4 Corneal aberrations. Diameter analysis is not the same and this affects the RMS values [17–20]

	Vinciguerra <i>n</i> = 1000; diameter = 5 mm; EyeTop	Wang <i>n</i> = 228; diameter = 6 mm Atlas	Zheleznyak <i>n</i> = 40; diameter = 5 mm Orbscan	Nur Colak <i>n</i> = 81; diameter = 6 mm; Sirius
HOA (μm)	0.16 ± 0.06	0.48 ± 0.12	0.29 ± 0.1	0.36 ± 0.1
Spherical (μm)	0.15 ± 0.05	0.28 ± 0.08	0.15 ± 0.09	0.22 ± 0.05
Coma (μm)	0.14 ± 0.08	0.25 ± 0.13	0.15 ± 0.08	0.48 ± 0.09
Trifoil (μm)	n.d.	n.d.	0.14 ± 0.09	0.13 ± 0.04

is that there is not very good agreement in corneal HOA measurements among devices [16]. It is important to know the normal range of the tomographer in use. Table 15.4 shows some references in normal eye samples. In our practice, we refrain from implanting multifocal IOLs when the HOA RMS value is three standard deviations away from the mean value.

Corneal Anatomical Quality

Corneal topography can detect surface pathology that can affect the optical performance of the pseudophakic eye and is a valuable tool for evolutionary follow up. A frequent situation is epithelial basement membrane dystrophy (EBMD) where corneal epithelial irregularities can alter central corneal power over time and lead to biometric error [21]. Surgery and post-surgical treatments can trigger epithelial changes that finally disturb the corneal surface. Corneal topography can detect and quantify central irregularity. The epithelial map available in some OCT tomographers is a powerful tool to diagnose this sort of pathology. A focal thickening is a characteristic feature in this map with values over $60 \mu\text{m}$. In the cross-sectional OCT image sometimes, an intraepithelial white nodule can be seen (Fig. 15.9).

Surface irregularity is a habitual feature of dry eye disease that also affects both optical performance of the pseudophakic eye and keratometry precision and accuracy [13]. It is a recognized source of dissatisfaction in patients with multifocal IOLs; therefore, it should always be taken into consideration in candidates for this type of

lens [22]. In addition to curvature and epithelial maps, some topographers can perform the NIBUT test (non-invasive break-up time), dynamic tear study and non-contact meibography. This can be completed by tear meniscus measurement with OCT which has shown to be a reliable diagnostic test [23].

Topographies of contact lens users must be examined carefully looking for any irregularity that can yield a keratometric and, consequently, an IOL power error. If this is the case, biometry should be repeated after the situation has cleared. Figure 15.10 shows a case with mild asymmetric keratometric astigmatism. The patient had stopped wearing soft contact lenses 10 days before. One month later the steepening of the superior semi-meridian had disappeared, the Sim K had flattened 1.05 D and keratometric astigmatism had reduced by 1.30 D.

In modern IOL surgery, patient expectations are very high and the final goal is to achieve a refractive status of emmetropia with the best possible uncorrected vision. The odds of needing some excimer treatments are around 5–10%, especially if multifocal IOLs are implanted where tolerance to any residual ametropia is very low. Any sign of subclinical corneal ectasia can lead to the contraindication of excimer laser surgery, and this can alter the surgical plan. Corneal tomography has boosted the detection of subclinical keratoconus by epithelium and pachymetry and analysis. The earliest morphological feature in keratoconus is a focal stromal thinning, usually in the inferior-temporal quadrant, with epithelium thinning, which is thought to be a compensating phenomenon that decreases the optical impact of the anterior protrusion [24].

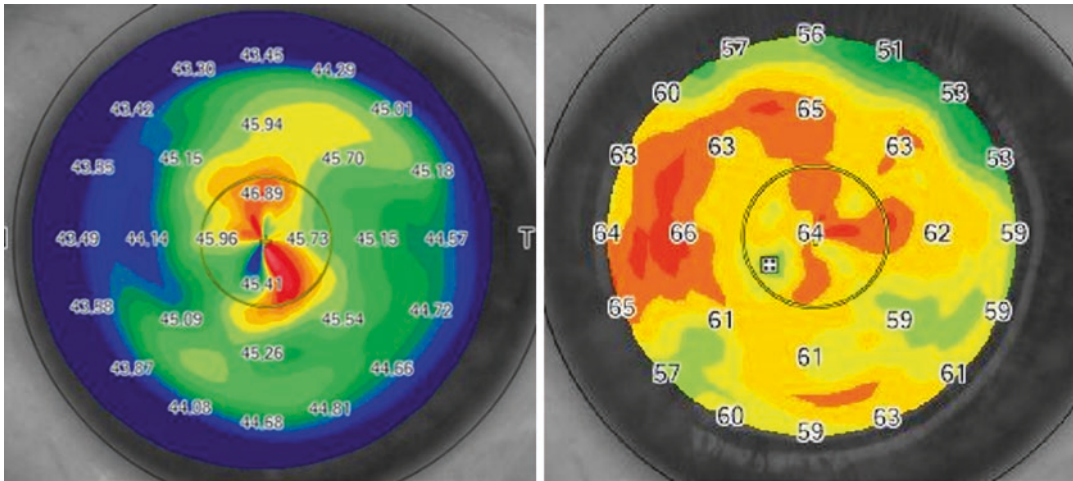


Fig. 15.9 Central corneal topographic irregularity in a case of epithelial basement membrane dystrophy. The epithelial map shows central irregular thickening

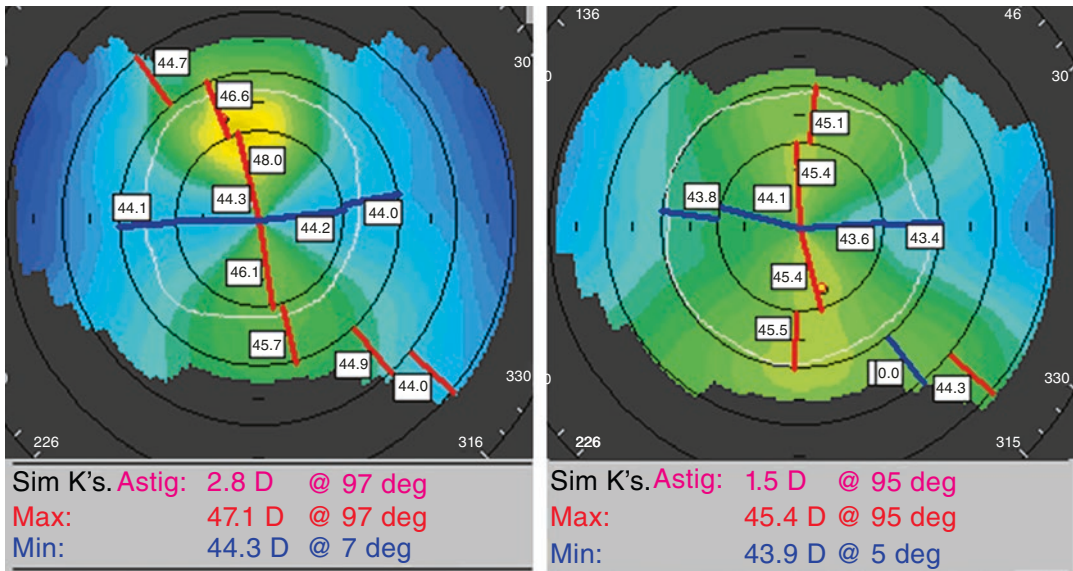


Fig. 15.10 Topographic and keratometric changes after discontinuing soft contact lenses. On the left, 10 days without contact lenses and on the right 1 month later

This is why the posterior elevation value is always higher than anterior. The epithelial map provided by some OCT tomographers can detect this pattern distinguishing it from other clinical entities, for example, epithelium focal hyperplasia rendering a pseudokeratoconic topographic pattern (Fig. 15.11).

The rate of corneal thickening from the thinnest point to the periphery is higher in the kera-

toconic cornea. This relevant feature was found by Ambrosio who developed two graphs in order to detect it: CTSP (corneal thickness spatial profile) and PTI (percentage thickness increase) [25].

Most topo-tomographers incorporate software modules dedicated to keratoconus diagnosis that help the clinician in the detection of this condition.

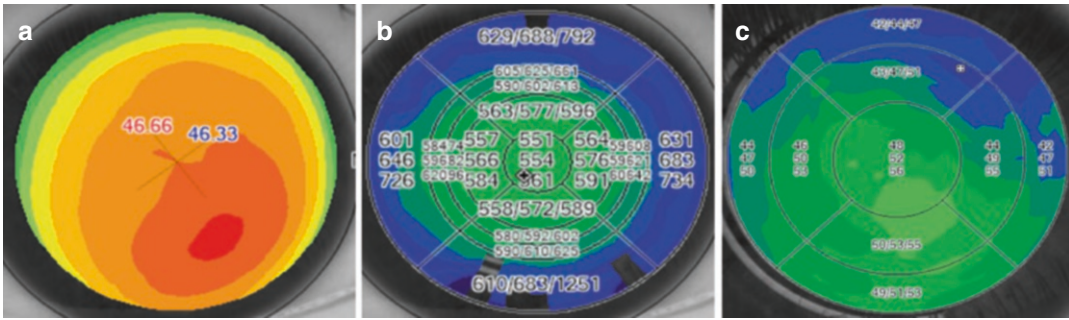


Fig. 15.11 (a) Possible keratoconus pattern in the axial keratometric map (left). (b) Pachymetry map looks normal (center). (c) There is epithelium thickening in the epi-

thelial map coincident with the steepened area: pseudoectasia produced by surface pathology

IOL Power Calculation

IOL power has been calculated for many years using optical vergence thin lens formulas. The corneal power parameter, essential in this calculation, has been provided by the keratometer in the form of a K value, which is calculated from the measured mean paracentral curvature radius applying the SKIR (1.3375) to account for the unmeasured posterior corneal power (see section “Measurements” above in this chapter). Since the first topographers, and now the tomographers, a similar value is calculated from an equivalent central corneal area, around 3 mm in diameter. This value is called Sim K (simulated keratometry) and can be used in the IOL calculation formulas as the agreement with K is fairly good. K does not correspond to any classic Gaussian optics definition. Although it approximates the corneal posterior vertex power, the reference plane is a little posterior to this [26].

Since corneal topographers can measure many points of the anterior surface and tomographers can measure the posterior surface curvature and power new options arise to parameterize corneal optics in order to calculate the IOL.

Important Concepts

- The actually measured area depends on curvature radius and asphericity. The steeper the cor-

nea, the smaller the measured area and vice versa. Corneal asphericity will finally determine if K is over or underestimated. In a very flat physiologically prolate cornea, K will be underestimated because the more peripheral curvature is smaller. On the contrary, in a very flat post-LASIK oblate cornea, K will be overestimated because the more peripheral curvature is higher (Fig. 15.12). This overestimation can be very significant if the shape factor is high.

- The accuracy of corneal power calculated with the SKIR depends on a certain ratio between the anterior and posterior corneal curvatures. The so-called Gullstrand ratio, whose normal value is: anterior radius/posterior radius = 1.21 ± 0.02 [9]. If it is expressed inversely: posterior radius/anterior radius = 0.82 ± 0.02 . In corneas, where this proportion is different, corneal power (K) will be miscalculated. If the ratio increases, there will be an overestimation of K value because the calculation will miss the relative anterior flattening effect. This happens after myopic LASIK/PRK [27], keratoconus [28], and DSAEK [29], to mention some frequently found conditions. If the ratio decreases, there will be an underestimation of K value because the calculation will miss the relative steepening effect. This happens after hyperopic LASIK/PRK, some presby-LASIK profiles and radial keratotomy (RK) [30] (Fig. 15.13). K values changes approximately five times the

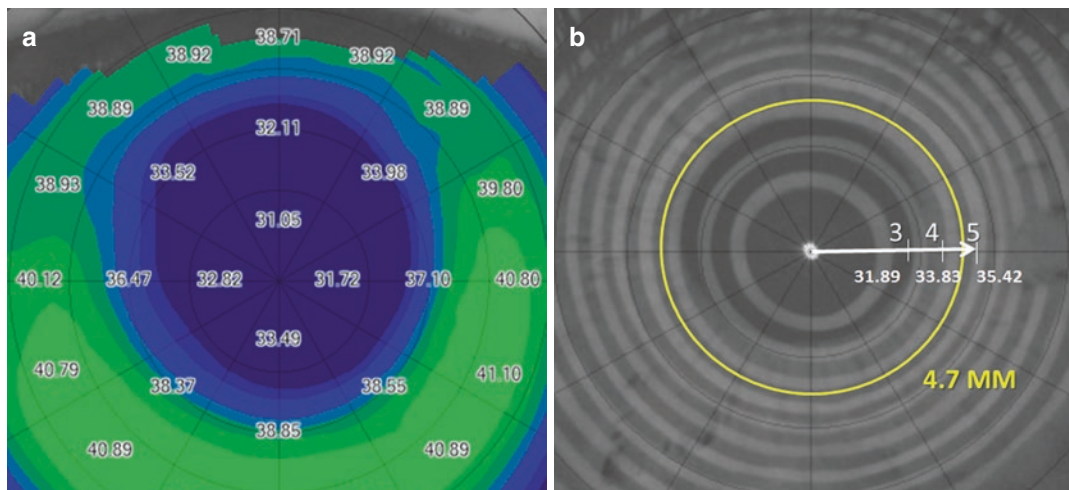
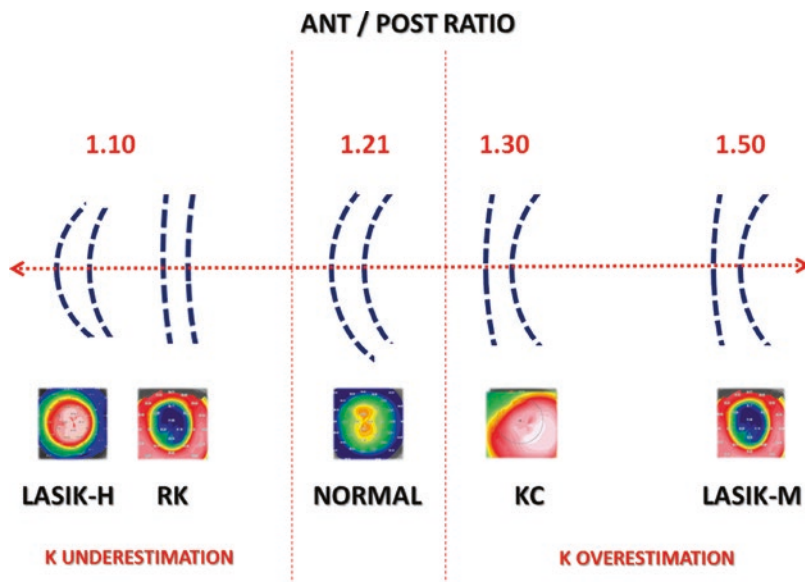


Fig. 15.12 Placido topography after LASIK-M. (a) The actually measured area diameter is 4.7 mm due to corneal curvature and shape. (b) Curvature gradient is very high as it can be seen in three reference positions: 3, 4, and 5 mm

Fig. 15.13 Anterior/posterior corneal ratio. Normality range is within red dotted lines. Central line scale is not proportional



corneal ratio change, for example, 0.3 corneal ratio converts to 1.5 in *K*.

Ant/post ratio change is proportional to the anterior curvature change produced by the laser in excimer surgery. This explains why a function can be fit to predict the effect (e.g., Haigis-L and Barrett true *K* formulas). While there is no such proportionality after RK and similar surgeries, the same number of cuts can produce different

effects on this ratio [30]. The accuracy of any predicting function will be worse by definition.

Parameters for IOL Calculations

Sim *K*

It can be used in any formula that requires a keratometric *K* value. In our practice, we use it as a double check of the keratometer measurement.

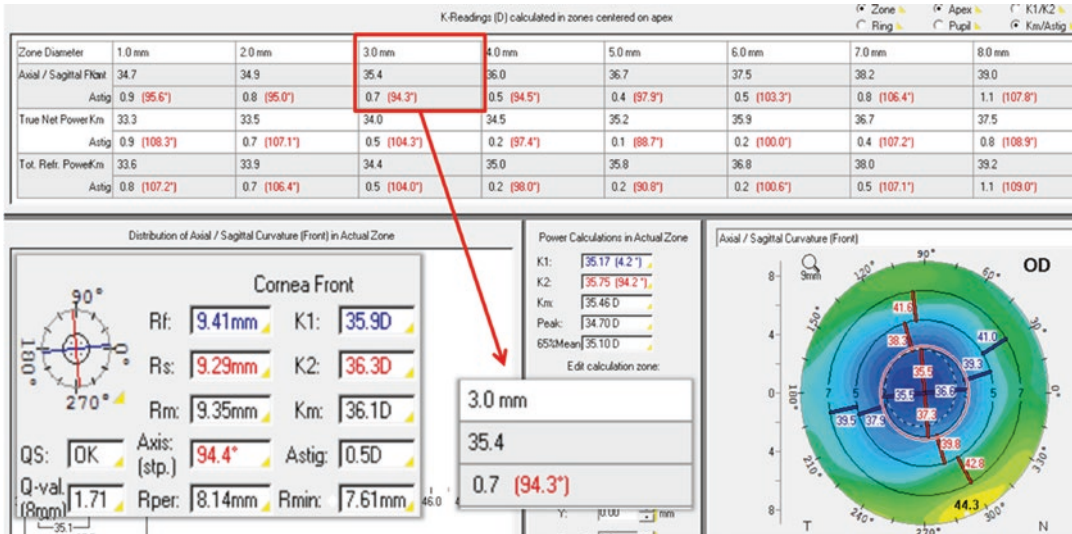


Fig. 15.14 Power distribution map in Pentacam. Post LASIK-M case. 36.1 D Sim K value becomes 35.40 D once adjusted to the 3 mm area in the Axial/sagittal front option

We know the bias between both devices from previous home-made agreement study.

In case of curvature and shape extreme values, the measurement area should be adjusted. This is particularly important in very flat and oblate corneas after LASIK/PRK and RK. The way to proceed depends on the topographer model. For example, with the Pentacam it can be done in the power distribution map module, adjusting the area of analysis to 3 mm of the parameter axial/sagittal curvature front (Fig. 15.14). In the Sirius and MS39, the Sim K option is changed by Meridians in the Indices table. The mean value for 3 mm will be the adjusted new *K*.

Equivalent K Reading (EKR)

Described first by Holladay for the Pentacam®, it can be defined as the total central power calculated from both measured anterior and posterior surfaces and adjusted to a reference plane similar to the keratometric *K* value [31]. Therefore, it can be used in any IOL power calculation formula designed to input *K* as the corneal parameter avoiding the ant/post ratio induced error. In a normal eye, this value should be very similar to Sim *K*, with just some difference from the variance of this ratio in the normal eye (SD = 0.02). In the

Pentacam®, the recommended value is EKR 4.5 mm which shows a 95% agreement range with keratometer measured *K* of 1.48 D [32]. However, there is some controversy on the results obtained with the EKR, both in normal and previously operated eyes [31–33]. In cases of DSAEK, Xu reported the lowest predictive error with EKR: -0.05 ± 1.02 D, achieving a good compensation for the altered ant/post ratio [29].

EKR is also available in the Cassini® software. We obtained good results using it with the Haigis formula in a series of 26 eyes after myopic LASIK with a mean ant/post ratio of 1.31 ± 0.06 . The predictive error was -0.16 ± 0.73 D, which is comparable to other published series (presented at the IOL Power Club meeting in Athens in 2017).

The Galilei® has a conceptually similar index called TCPIOL calculated by ray-tracing and referenced to the posterior corneal surface in order to equal Sim *K*, but it does not seem to improve the results in normal eyes [34].

Total Corneal Power

All tomographers calculate a central corneal power parameter by ray tracing through the anterior and posterior surfaces normally using the

Gullstrand values for the index of refraction of cornea (≈ 1.376) and aqueous (≈ 1.336). This measurement has been given different names: It is called total corneal refractive power (TCRP) in the Pentacam®, total corneal power (TCP) in the Galilei® and Anterior®, real power in the Casia® and Revo NX®, and mean pupilar power (MPP) in the Sirius® and MS39®. It should be pointed out that the Galilei® presents three different values: TCP1, TCP2, and TCP-IOL, depending on the index of refraction used and the corneal reference plane (see the Galilei® chapter in this book).

Some tomographers offer alternatively a K value calculated using the Gaussian equivalent power formula:

$$P = K_{\text{ant}} + K_{\text{post}} - \left(\frac{d}{n} \right) * K_{\text{ant}} * K_{\text{post}} \quad (15.2)$$

where P is power, K_{ant} is the anterior corneal power, K_{post} is the posterior corneal power calculated using Eq. (15.1), d is corneal thickness, and n is corneal refractive index. In the Pentacam®, this value is called true net power (TNP).

All these powers have reference planes anterior to the Sim K and thus have lower dioptric values. Although they all share the interesting feature of taking into account the posterior measured curvature and avoiding the proportion assumption of the Sim K, they cannot be directly input into regular IOL formulas as these are designed for the Sim K. Internally, the formula converts the K to a more accurate value using another corneal refractive index that will be between 1.3215 and 1.3333 depending on the formula [35]. However if a new IOL constant is calculated specifically for any of these values results can be correct both in normal eyes and post-corneal refractive surgery IOL power calculations [34, 36]. This new IOL constant will correct the bias between the total corneal power and the Sim K.

Radii of Curvature

A simple way of avoiding this K confusion is using the radii of curvature values in mm that all formulas allow as input. It also prevents from any error in the adjustment of the keratometry index of refraction.

Central Corneal Elevation Data

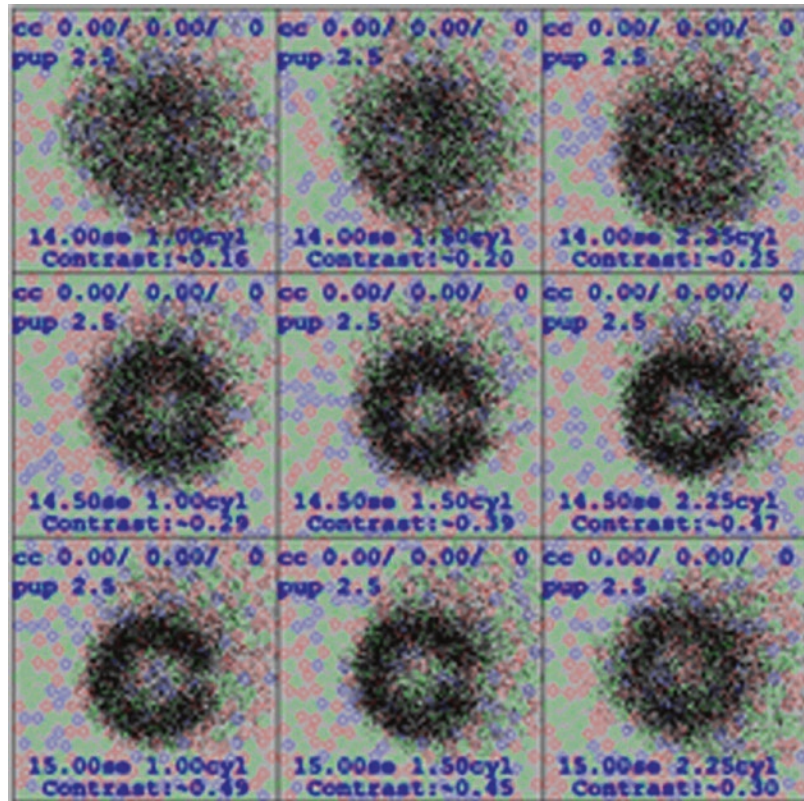
The cornea can be represented by a topographic data matrix which will be implemented in an exact ray-tracing eye model in order to calculate the optical performance of the pseudophakic eye. It can be done just using the anterior corneal surface but accuracy will certainly be better if the posterior cornea is represented in the same way by a tomographer. This will take account of HOAs and the best IOL power, both in terms of spherical equivalent and toricity and can be selected regarding different visual optical metrics beyond spectacle refraction as optimization factor. This methodology should provide better outcomes than paraxial methods whenever the amount of HOA is high.

Okulix software works in this way and is available in different biometry and topography devices (Fig. 15.15). It can also perform paraxial calculations based on indices (Sim K). The exact ray-tracing mode does not seem to offer any advantage in normal eyes over regular formulas or over the paraxial calculation by the same software. However, it has been shown to be a very good option after corneal refractive surgery: Savini reported 63.6% of cases within ± 0.50 D of the target [36]. Results might be even better if measurements are obtained with a SS-OCT device: Gjerdrum et al. have found excellent outcomes with Anterior® and Okulix: PE within ± 0.5 D in 88% of eyes [37].

The tomographers Sirius® and MS39® have a software module that performs IOL calculations by exact ray-tracing. The IOL position is estimated with a proprietary algorithm using several anterior segment parameters as predictors. Savini et al. reported 71% of eyes within ± 0.50 D of prediction with Sirius [14] and 75% of eyes in a non-published series with the MS 39 instrument using optical-segmented AL.

Our group calculates the irregular cornea cases, mainly post-refractive and keratoconus, exporting the corneal elevations from the tomographer to Zemax® optical design software, first performing a 3D model with an algorithm programmed in Matlab®, and selecting the IOL power based on an optimizing function with the through-focus visual Strehl metrics which has a

Fig. 15.15 Simulation of Landolt C image with different IOL powers. The effect of HOA is considered and the IOL that produces the best quality image should be the best option



good correlation with the subjective refraction [38] (Fig. 15.16). At the 2021 IOL Power Club meeting, we presented a series of 75 eyes post-LASIK where 78.4% of eyes were ± 0.50 D of predicted refraction (SE), and these values were 84% and 83% for J0 and J45 vectors, respectively.

Corneal Asphericity and Spherical Aberration

IOL designs have different shape factors to compensate the spherical aberration of the cornea. Hence, it is useful to know this value in the cornea to aim for a certain target, either zero or not. This can be particularly relevant in situations like keratoconus or after corneal refractive surgery where spherical aberration can be very high and impair visual quality.

All topo-tomographers measure corneal asphericity expressing this value in any of the well-defined coefficients: Q , p , e , and E . More useful is the spherical aberration measurement, in

μm , obtained from the wavefront error Zernike polynomial expansion, that can be found in the IOL calculation menu and in the Wavefront analysis menu. The spherical aberration Zernike coefficient is the C12 or $Z(4, 0)$. It is a general consensus in refractive surgery to measure this value for 6 mm analysis diameter.

It should be remarked that the objective is the spherical aberration (anterior + posterior) and not the asphericity. This will yield a different spherical aberration depending on the radius of curvature: The higher the curvature, the higher the induced spherical aberration for a constant asphericity value [39].

Axis of Reference

All topographers measure the distance between two cardinal references: pupil center and corneal vertex. Although there is some terminology confusion about these axes, they are usually named angle kappa (in degrees) and distance chord μ (in mm). Several reports have found a relationship

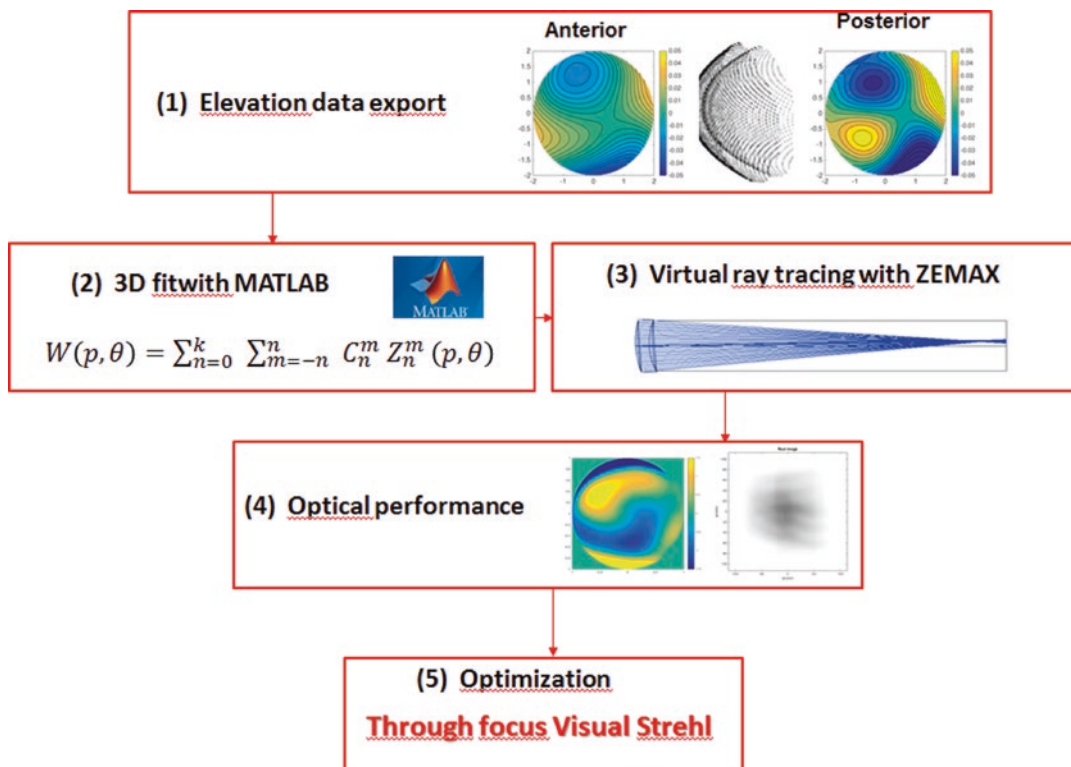


Fig. 15.16 IOL calculation from corneal elevations. Flow chart

between these values and the optical quality and patient satisfaction with different types of IOLs. Large angle kappa is related to higher risk of unwanted photic phenomena with multifocal IOLs [40, 41]. Therefore, measuring these values can be useful to select the type of IOL and properly center the capsulorrhexis and the IOL.

Toric IOL Calculation

Many studies show that the prevalence of significant corneal astigmatism is high with 30–43% of corneas presenting more than 1 D of keratometric astigmatism. Vision degradation is relevant over this value and can be a practical threshold to indicate the implantation of a toric IOL [42]. Corneal topo-tomography is the cornerstone in corneal astigmatism quantitative and qualitative analysis and, therefore, the essential tool in toric IOL selection.

Regular and Irregular Astigmatism

Regular astigmatism occurs if the refracting toric surface has two orthogonal meridians with geometrically identical semi-meridians. The curvature topographic feature will be a symmetric bowtie. The size and the color distribution of this bowtie will depend on corneal shape and curvature. As the shape gets more prolate, the bowtie becomes smaller and the steep axis stands out (Fig. 15.17).

Irregular astigmatism can also be defined as the presence of HOA. With regular toric IOLs, only regular astigmatism can be fully corrected. However, with advanced optic calculations there is room for IOL selection in order to achieve some compensation of the HOA. Frequent cases of irregular astigmatism are: post-LASIK/PRK/RK corneas, keratoconus, scars, etc. In very aberrated corneas paraxial calculations are non-sense and topography data-based calculations should

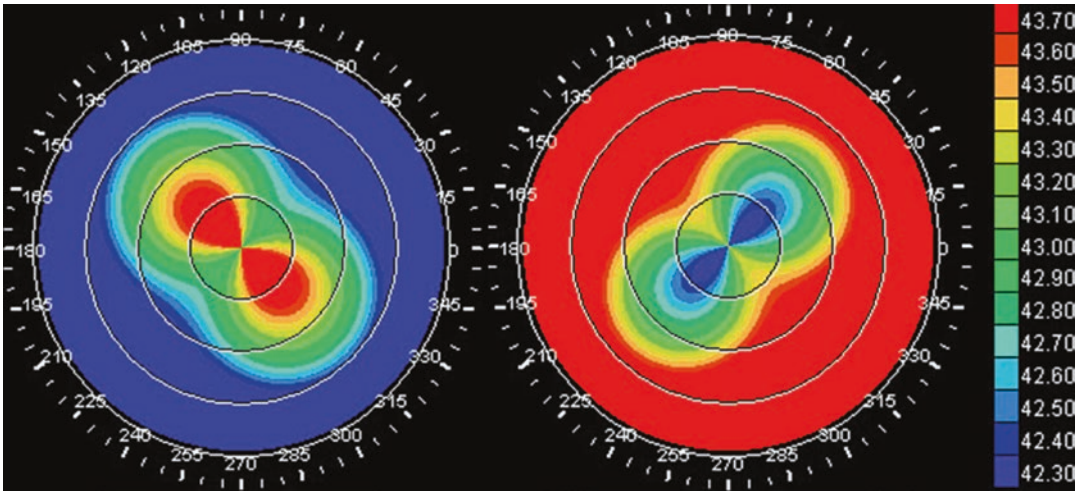


Fig. 15.17 Axial map simulation: Same astigmatism in both cases with apical radii 8.00 and 7.8 mm. The only difference is the shape factor. Left image is prolate

($p = 0.75$), and right image is oblate ($p = 1.25$). The prominent meridian is the steep one in the first case and the flat one in the second

be done using a ray-tracing method on a thick lens model. In Fig. 15.18, a very aberrated cornea that had undergone RK years before was calculated with a ray-tracing software obtaining an accurate refractive prediction.

Measured and Estimated Total Astigmatism

Keratometric astigmatism (K and Sim K) estimates total corneal astigmatism using the SKIR, 1.3375, value, which assumes a normal anterior/posterior corneal ratio and symmetry between steep-flat meridians in both surfaces. Since corneal tomographers can measure the posterior cornea, it has become evident that this is not always true. Koch et al. measured 715 corneas with the Galilei[®] and found that the steep meridian was vertical in 51.9% of anterior surfaces and 86.6% of posterior ones. This discrepancy means that keratometric astigmatism tends to overestimate with-the-rule (WTR) astigmatism and underestimate against-the-rule (ATR) astigmatism. The mean error vector was 0.22 D a 180°. In 5% of cases, the error was higher than 0.50 D [43]. Savini et al. reported similar findings with the Sirius[®] in 157 eyes. Sim K astigmatism overesti-

mated WTR astigmatism, 0.22 ± 0.32 D, underestimated ATR, 0.21 ± 0.26 D, and overestimated the oblique, 0.13 ± 0.37 D. In this study, there was a difference higher than 0.50 D between keratometric astigmatism and total astigmatism in 16% of cases [44]. Therefore, corneal total astigmatism, as measured from both the anterior and posterior corneal surfaces with a tomographer, is better than keratometric astigmatism as a toric IOL target. All tomographers display this value in the total corneal power analysis. This value can also be found in the total cornea wavefront error analysis, where the common vector for $Z(2, 2)$ and $Z(2, -2)$ in an area of 3 mm should be a very similar value (Fig. 15.19).

However, published evidence shows that empirical formulas that estimate the target total astigmatism from the keratometric astigmatism yield more accurate toric IOL calculations than the total corneal astigmatism mentioned in the previous paragraphs. Some of the most used formulas are: Barrett Toric, Abulafia-Koch, Holladay 2 Toric Naeser-Savini, Kane Toric, etc. [45, 46].

It has been proposed that IOL tilt can be the source for that residual astigmatism that cannot be predicted from the corneal measurements. It seems that IOL tilt can be estimated from preoperative lens tilt. If this is so, the incorporation of

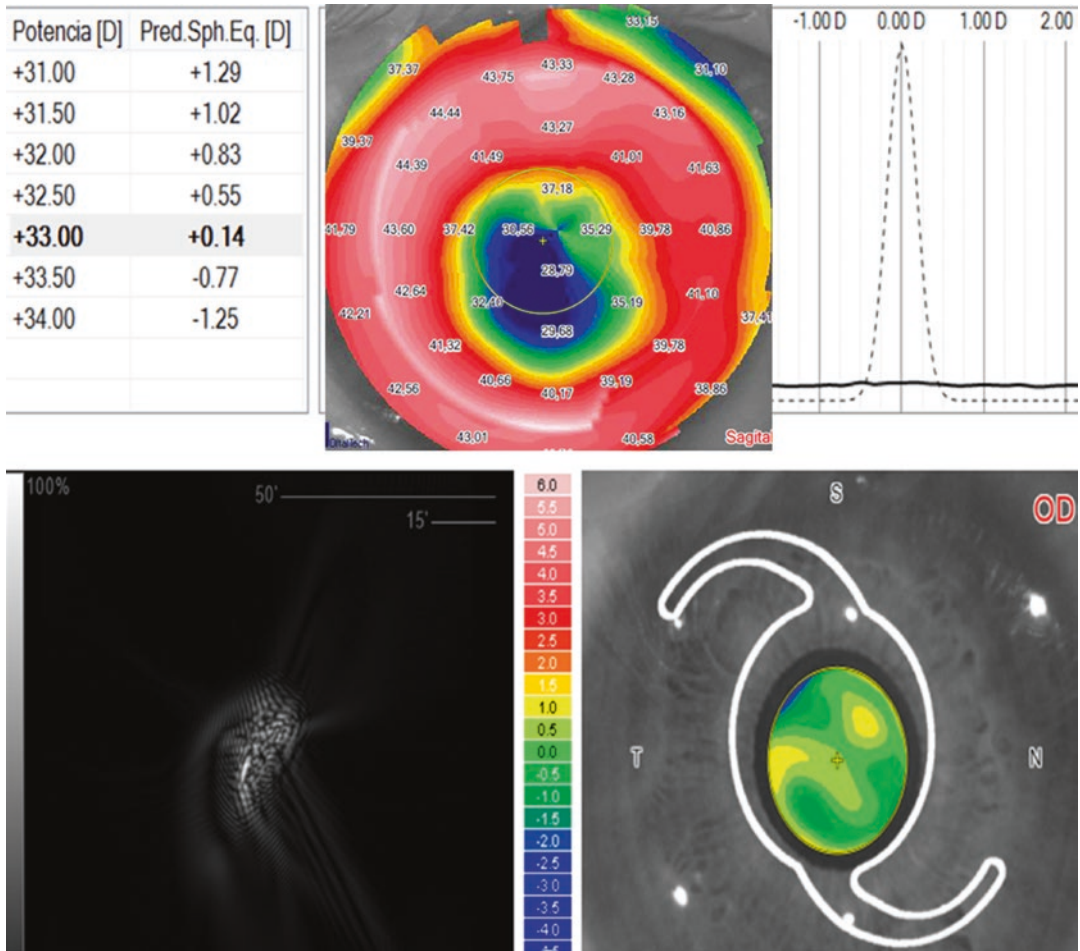


Fig. 15.18 Decentered and small optical zone after RK. AL = 24.63 mm; K (Lenstar): 31.87/33.53 D. Ray-tracing calculation (MS39) predicts +0.14 D refraction with +33.00 IOL power. After surgery subjective residual refraction was plano. PSF and wavefront error graphics display the bad visual quality of this eye

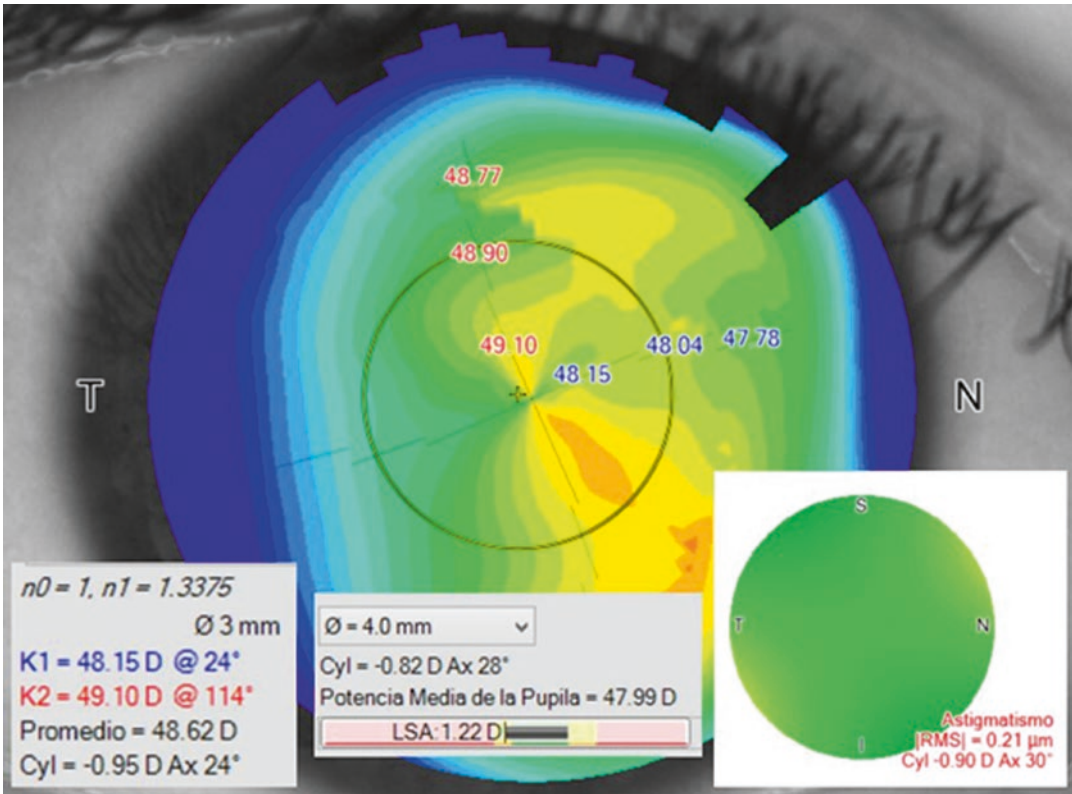


Fig. 15.19 Corneal tomography. Keratometric astigmatism is -0.95 D a 24° , total astigmatism is -0.82 D a 28° and total aberrometric astigmatism (3 mm) is -0.90 D a 30°

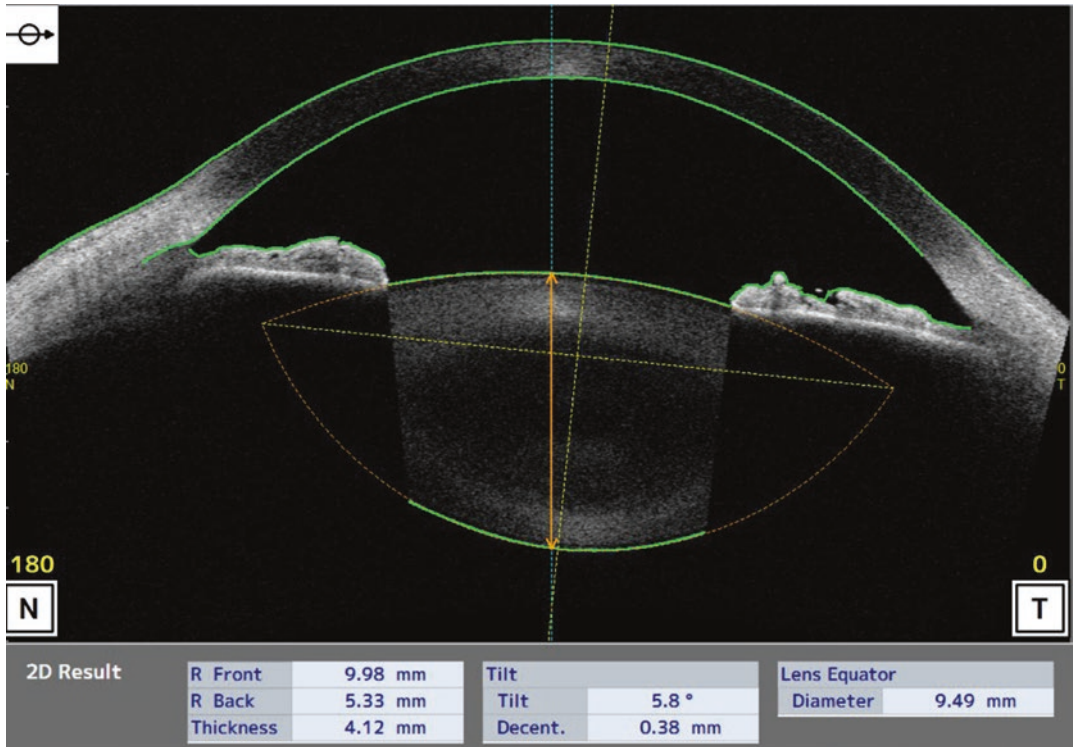


Fig. 15.20 Natural lens analysis with CASIA 2: curvatures, thickness, and tilt are measured

this variable in a theoretical model might improve results in the near future. SS-OCT tomographers can measure the tilt of the natural lens (Fig. 15.20) [47, 48].

References

- Gills JP, et al. Corneal topography: the state of the art. Thorofare, NJ: Slack Incorporated; 1995. p. 1–328.
- Ventura BV, Al-Mohtaseb Z, Wang L, Koch DD, Weikert MP. Repeatability and comparability of corneal power and corneal astigmatism obtained from a point-source color light-emitting diode topographer, a Placido-based corneal topographer, and a low-coherence reflectometer. *J Cataract Refract Surg.* 2015;41(10):2242–50.
- Kaschke M, Donnerhacke K-H, Rill MS. Optical visualization, imaging, and structural analysis. In: *Optical devices in ophthalmology and optometry*. 1st ed. Weinheim: Wiley-VCH; 2014.
- Mattioli R, Carones F, Cantera E. New algorithms to improve the reconstruction of corneal geometry on the keratron videokeratographer. *Invest Ophthalmol Vis Sci.* 1995;36(Suppl):1400.
- Klein SA. Axial curvature and the skew ray error in corneal topography. *Optom Vis Sci.* 1997;74(11):931–44.
- Cairns G, McGhee CN. Orbscan computerized topography: attributes, applications, and limitations. *J Cataract Refract Surg.* 2005;31(1):205–20.
- Wang SB, Cornish EE, Grigg JR, McCluskey PJ. Anterior segment optical coherence tomography and its clinical applications. *Clin Exp Optom.* 2019;102(3):195–207.
- Szalai E, Berta A, Hassan Z, et al. Reliability and repeatability of swept-source Fourier-domain optical coherence tomography and Scheimpflug imaging in keratoconus. *J Cataract Refract Surg.* 2012;38(3):485–94.
- Aramberri J, Araiz L, Garcia A, Illarramendi I, Olmos J, Oyanarte I, Romay VI. Dual versus single Scheimpflug camera for anterior segment analysis: precision and agreement. *J Cataract Refract Surg.* 2012;38:19341949.
- Corbett MC, Rosen ES, O’Brart DPS. Assessment of corneal shape. In: *Corneal topography. Principles and applications*. 1st ed. London: BMJ Books; 1999.
- Calossi A. Corneal asphericity and spherical aberration. *J Refract Surg.* 2007;23(5):505–14.
- Savini G, Schiano-Lomoriello D, Hoffer KJ. Repeatability of automatic measurements by a new anterior segment optical coherence tomographer combined with Placido topography and agreement

- with 2 Scheimpflug cameras. *J Cataract Refract Surg.* 2018;44(4):471–8.
13. Epitropoulos AT, Matossian C, Berdy GJ, Malhotra RP, Potvin R. Effect of tear osmolarity on repeatability of keratometry for cataract surgery planning. *J Cataract Refract Surg.* 2015;41:1672–7.
 14. Savini G, Bedei A, Barboni P, Ducoli P, Hoffer KJ. Intraocular lens power calculation by ray-tracing after myopic excimer laser surgery. *Am J Ophthalmol.* 2014;157:150–3.
 15. Goto S, Maeda N. Corneal topography for intraocular lens selection in refractive cataract surgery. *Ophthalmology.* 2020;19. pii: S0161-6420(20)31108-8.
 16. Piccinini AL, Golan O, Hafezi F, Randleman JB. Higher-order aberration measurements: comparison between Scheimpflug and dual Scheimpflug-Placido technology in normal eyes. *J Cataract Refract Surg.* 2019;45(4):490–4.
 17. Vinciguerra P, Camesasca FI, Calossi A. Statistical analysis of physiological aberrations of cornea. *J Refract Surg.* 2003;19:S265–9.
 18. Wang L, Dai E, Koch DD, Nathoo A. Optical aberrations of the human anterior cornea. *J Cataract Refract Surg.* 2003;29:1514–21.
 19. Zheleznyak L, Kim MJ, MacRae S, Yoon G. Impact of corneal aberrations on through-focus image quality of presbyopia-correcting intraocular lenses using an adaptive optics bench system. *J Cataract Refract Surg.* 2012;38(10):1724–33.
 20. Colak HN, Kantarci FA, Yildirim A, et al. Comparison of corneal topographic measurements and high order aberrations in keratoconus and normal eyes. *Cont Lens Anterior Eye.* 2016;39:380–4.
 21. Ho WM, Stanojic N, O'Brart N, O'Brart D. Refractive surprise after routine cataract surgery with multifocal IOLs attributable to corneal epithelial basement membrane dystrophy. *J Cataract Refract Surg.* 2019;45:685–9.
 22. Gibbons A, Ali TK, Waren DP, Donaldson KE. Causes and correction of dissatisfaction after implantation of presbyopia-correcting intraocular lenses. *Clin Ophthalmol.* 2016;10:1965–70.
 23. Chan HH, Zhao Y, Tun TA, Tong L. Repeatability of tear meniscus evaluation using spectral-domain Cirrus® HD-OCT and time-domain Visante® OCT. *Cont Lens Anterior Eye.* 2015;38(5):368–72.
 24. Reinstein DZ, Archer TJ, Gobbe M. Corneal epithelial thickness profile in the diagnosis of keratoconus. *J Refract Surg.* 2009;25(7):604–10.
 25. Ambrosio R Jr, Caiado AL, Guerra FP, et al. Novel pachymetric parameters based on corneal tomography for diagnosing keratoconus. *J Refract Surg.* 2011;27:753–8.
 26. Wang L, Mahmoud AM, Anderson BL, Koch DD, Roberts CJ. Total corneal power estimation: ray tracing method versus gaussian optics formula. *Invest Ophthalmol Vis Sci.* 2011;52(3):1716–22.
 27. Seitz B, Torres F, Langenbucher A, et al. Posterior corneal curvature changes after myopic laser in situ keratomileusis. *Ophthalmology.* 2001;108:666–73.
 28. Tomidokoro A, Oshika T, Amano S, Higaki S, Maeda N, Miyata K. Changes in anterior and posterior corneal curvatures in keratoconus. *Ophthalmology.* 2000;107:1328–32.
 29. Xu K, Qi H, Peng R, Xiao G, Hong J, Hao Y, Ma B. Keratometric measurements and IOL calculations in pseudophakic post-DSAEK patients. *BMC Ophthalmol.* 2018;18:268.
 30. Camellin M, Savini G, Hoffer K, et al. Scheimpflug camera measurement of anterior and posterior corneal curvature in eyes with previous radial keratotomy. *J Refract Surg.* 2012;28:275–9.
 31. Holladay JT, Hill WE, Steinhilber A. Corneal power measurements using Scheimpflug imaging in eyes with prior corneal refractive surgery. *J Refract Surg.* 2009;25:862–8.
 32. Karunaratne N. Comparison of the Pentacam equivalent keratometry reading and IOL Master keratometry measurement in intraocular lens power calculations. *Clin Exp Ophthalmol.* 2013;41(9):825–34.
 33. Lam S, Gupta BK, Hahn JM, Manastersky NA. Refractive outcomes after cataract surgery: Scheimpflug keratometry versus standard automated keratometry in virgin corneas. *J Cataract Refract Surg.* 2011;37:1984–7.
 34. Savini G, Negishi K, Hoffer KJ, Lomoriello DS. Refractive outcomes of intraocular lens power calculation using different corneal power measurements with a new optical biometer. *J Cataract Refract Surg.* 2018;44:701–8.
 35. Holladay JT. Standardizing constants for ultrasonic biometry, keratometry, and intraocular lens power calculations. *J Cataract Refract Surg.* 1997;23:1356–70.
 36. Savini G, Hoffer KJ, Schiano-Lomoriello D, Barboni P. Intraocular lens power calculation using a Placido disk-Scheimpflug tomographer in eyes that had previous myopic corneal excimer laser surgery. *J Cataract Refract Surg.* 2018;44(8):935–41.
 37. Gjerdrum B, Gundersen KG, Lundmark PO, Aakre BM. Refractive precision of ray tracing IOL calculations based on OCT data versus traditional IOL calculation formulas based on reflectometry in patients with a history of laser vision correction for myopia. *Clin Ophthalmol.* 2021;15:845–57.
 38. Young LK, Love GD, Smithson HE. Accounting for the phase, spatial frequency and orientation demands of the task improves metrics based on the visual Strehl ratio. *Vis Res.* 2013;90:57–6.
 39. Holladay JT. Effect of corneal asphericity and spherical aberration on intraocular lens power calculations. *J Cataract Refract Surg.* 2015;41:1553–4.
 40. Fu Y, Kou J, Chen D, Wang D, Zhao Y, Hu M, Lin X, Dai Q, Li J, Zhao YE. Influence of angle kappa and angle alpha on visual quality after implantation of multifocal intraocular lenses. *J Cataract Refract Surg.* 2019;45(9):1258–64.

41. Karhanová M, Pluháček F, Mičák P, Vlácil O, Šín M, Marešová K. The importance of angle kappa evaluation for implantation of diffractive multifocal intraocular lenses using pseudophakic eye model. *Acta Ophthalmol.* 2015;93(2):e123–8.
42. Kessel L, Andresen J, Tendal B, et al. Toric intraocular lenses in the correction of astigmatism during cataract surgery: a systematic review and meta-analysis. *Ophthalmology.* 2016;123(2):275–86.
43. Koch DD, Ali SF, Weikert MP, et al. Contribution of posterior corneal astigmatism to total corneal astigmatism. *J Cataract Refract Surg.* 2012;38(12):2080–7.
44. Savini G, Versaci F, Vestri G, et al. Influence of posterior corneal astigmatism on total corneal astigmatism in eyes with moderate to high astigmatism. *J Cataract Refract Surg.* 2014;40(10):1645–53.
45. Ferreira TB, Ribeiro P, Ribeiro FJ, O'Neill JG. Comparison of methodologies using estimated or measured values of total corneal astigmatism for toric intraocular lens power calculation. *J Refract Surg.* 2017;33(12):794–800.
46. Kane JX, Connell B. A comparison of the accuracy of 6 modern toric intraocular lens formulas. *Ophthalmology.* 2020;127(11):1472–86.
47. Hirschall N, Buehren T, Bajramovic F, Trost M, Teuber T, Findl O. Prediction of postoperative intraocular lens tilt using swept-source optical coherence tomography. *J Cataract Refract Surg.* 2017;43(6):732–6.
48. Weikert MP, Golla A, Wang L. Astigmatism induced by intraocular lens tilt evaluated via ray tracing. *J Cataract Refract Surg.* 2018;44:745–9.

Open Access This chapter is licensed under the terms of the Creative Commons Attribution 4.0 International License (<http://creativecommons.org/licenses/by/4.0/>), which permits use, sharing, adaptation, distribution and reproduction in any medium or format, as long as you give appropriate credit to the original author(s) and the source, provide a link to the Creative Commons license and indicate if changes were made.

The images or other third party material in this chapter are included in the chapter's Creative Commons license, unless indicated otherwise in a credit line to the material. If material is not included in the chapter's Creative Commons license and your intended use is not permitted by statutory regulation or exceeds the permitted use, you will need to obtain permission directly from the copyright holder.

